AFRL-AFOSR-VA-TR-2021-0043

Data-Driven Modeling for Dual Retrospectve Cost Adaptive Control

Bernstein, Dennis
REGENTS OF THE UNIVERSITY OF MICHIGAN
503 THOMPSON ST
ANN ARBOR, MI, 48109
USA

06/01/2021
Final Technical Report

Air Force Research Laboratory
Air Force Office of Scientific Research
Arlington, Virginia 22203
Air Force Materiel Command

REPORT DOCUMENTATION PAGE

Form Approved
OMB No. 0704-0188

1. REPORT DATE *(DD-MM-YYYY)*	**2. REPORT TYPE**	**3. DATES COVERED** *(From - To)*
01-06-2021	Final	01 Apr 2018 - 31 Mar 2021

4. TITLE AND SUBTITLE
Data-Driven Modeling for Dual Retrospectve Cost Adaptive Control

5a. CONTRACT NUMBER

5b. GRANT NUMBER
FA9550-18-1-0171

5c. PROGRAM ELEMENT NUMBER

6. AUTHOR(S)
Dennis Bernstein

5d. PROJECT NUMBER

5e. TASK NUMBER

5f. WORK UNIT NUMBER

7. PERFORMING ORGANIZATION NAME(S) AND ADDRESS(ES)
REGENTS OF THE UNIVERSITY OF MICHIGAN
503 THOMPSON ST
ANN ARBOR, MI 48109
USA

8. PERFORMING ORGANIZATION REPORT NUMBER

9. SPONSORING/MONITORING AGENCY NAME(S) AND ADDRESS(ES)
AF Office of Scientific Research
875 N. Randolph St. Room 3112
Arlington, VA 22203

10. SPONSOR/MONITOR'S ACRONYM(S)
AFRL/AFOSR RTA2

11. SPONSOR/MONITOR'S REPORT NUMBER(S)
AFRL-AFOSR-VA-TR-2021-0043

12. DISTRIBUTION/AVAILABILITY STATEMENT
A Distribution Unlimited: PB Public Release

13. SUPPLEMENTARY NOTES

14. ABSTRACT
This final report summarizes progress on AFOSR grant FA9550-18-1-0171 between April 1, 2018 and March 31, 2021. This project contributed to the various extensions of retrospective cost adaptive control (RCAC). These extensions include 1) RCAC-based PID control, and 2) data-driven retrospective cost adaptive control (DRCAC), where online system identification is used to obtain the required modeling information. Numerical studies illustrating these methods include a model scramjet, aerodynamic flutter, and missile guidance.

15. SUBJECT TERMS

16. SECURITY CLASSIFICATION OF:			**17. LIMITATION OF ABSTRACT**	**18. NUMBER OF PAGES**	**19a. NAME OF RESPONSIBLE PERSON**
a. REPORT	**b. ABSTRACT**	**c. THIS PAGE**			ERIK BLASCH
U	U	U	UU	8	**19b. TELEPHONE NUMBER** *(Include area code)* 426-7311

Standard Form 298 (Rev.8/98)
Prescribed by ANSI Std. Z39.18

May 21, 2021

Dear Dr. Blasch,

I am pleased to submit the final report for AFOSR grant FA9550-18-1-0171 entitled *Data-Driven Modeling for Dual Retrospective Cost Adaptive Control*. This project provided the opportunity for my research group to extend our research on adaptive control for diverse DOD applications. We demonstrated new techniques on computational models of a scramjet, aerodynamic flutter, and missile guidance.

Thank you for your support and the opportunity to contribute to the DOD mission.

Sincerely,

Dennis S. Bernstein

Data-Driven Modeling for Dual Retrospective Cost Adaptive Control

FA9550-18-1-0171

Final Report
May 21, 2021

Dennis S. Bernstein, PI
Department of Aerospace Engineering
The University of Michigan
Ann Arbor MI, 48109-2140
(734) 764-3719
dsbaero@umich.edu

Grant Monitor:
Dr. Erik Blasch
AFOSR

Abstract

This final report summarizes progress on AFOSR grant FA9550-18-1-0171 between April 1, 2018 and March 31, 2021. This project contributed to the various extensions of retrospective cost adaptive control (RCAC). These extensions include 1) RCAC-based PID control, and 2) data-driven retrospective cost adaptive control (DRCAC), where online system identification is used to obtain the required modeling information. Numerical studies illustrating these methods include a model scramjet, aerodynamic flutter, and missile guidance.

1 Overview of the Project

Retrospective cost adaptive control (RCAC) was developed at the University of Michigan [1–3], and has been applied to aircraft, spacecraft, and acoustic systems. For example, a detailed study of emergency flight control is given in [4].

The objective of this project was to extend RCAC in order to reduce the need for prior modeling information; we call this data-driven RCAC (DRCAC). DRCAC is needed to aimed at highly challenging applications, such as control of unstart in scramjets, which involve complex physics that are extremely different to model in advance of operation.

To achieve this objective, we are focusing on two key extensions of RCAC, namely, 1) augmentation of RCAC to address asymptotic constraints, and 2) RCAC with concurrent real-time model identification.

2 Research Accomplishments

2.1 Enforcing Asymptotic Output Constraints

As a first step toward enforcing output constraints, we note that enforcing constraints is closely related to conflicting commands. In particular, suppose that minimizing an error metric leads to violation of a constraint on the same or a different signal. Enforcing the constraint can then be viewed as issuing a conflicting command, namely, to minimize one signal while constraining the other signal.

To take advantage of this idea, we apply RCAC to the problem of following conflicting commands. In particular, the single output $y(k)$ is simultaneously requested to simultaneously follow different commands, which is of course impossible. In this case, it is observed that RCAC produces a controller such that the output $y(k)$ of the system follows a linear combination of the conflicting commands, where the linear combination is determined by the chosen weights in RCAC. RCAC with asymptotic constraints was applied to prevent unstart in a 2D scramjet combustor in [5].

As an example, consider the spring-mass-damper system

$$m\ddot{x} + c\dot{x} + kx = u, \tag{1}$$

where x is the position of the particle with mass m, the c is damping coefficient, k is the spring stiffness, and u is the applied input. Let the measured output be $y(k) = x(kT_{\mathrm{s}})$, where $T_{\mathrm{s}} = 0.01$ sec is the sampling time. The conflicting commands are chosen to be the setpoints $r_1(k) = 1$ and $r_2(k) = 2$. RCAC is implemented with $N_1 = [1\ 1]^{\mathrm{T}}$, $R_z = I_2$, $R_\theta = 10^2 I_{l_\theta}$, and $\lambda = 0.999$. Figure 1 shows the closed-loop response of the spring-mass-damper system

with conflicting commands, (a) shows the measured output $y(k)$, (b) shows the control $u(k)$, (c) shows the output error $z(k)$, and (d) shows the coefficients of the controller optimized by RCAC. Note that the output converges to the mean of the commands.

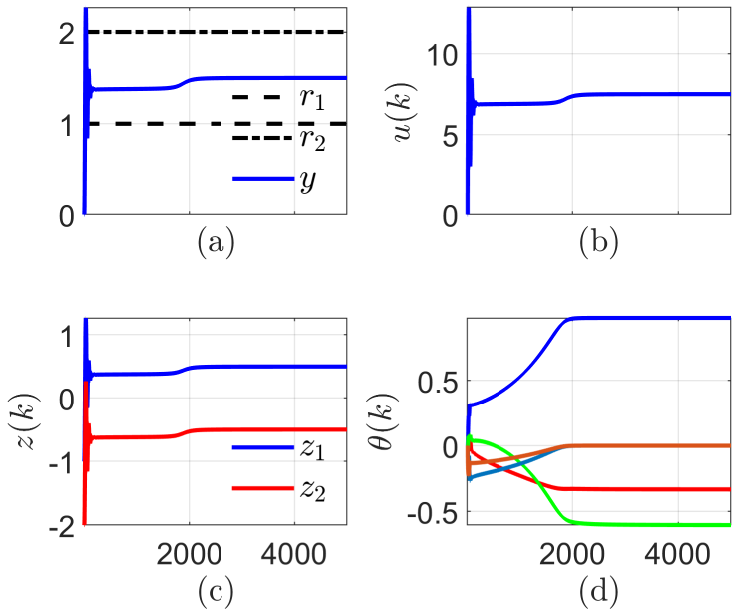

Figure 1: Closed-loop response of the spring-mass-damper system with conflicting commands. Note that the output converges to the mean of the conflicting commands.

Next, RCAC is applied to the problem of following commands to the scramjet. The conflicting commands are assumed to be less than the critical thrust at the operating conditions, where the critical thrust is the largest value of thrust the scramjet can generate at steady state at the given operating condition. In particular, the scramjet is commanded to follow the step commands $r_1(k) = 0.24$ and $r_2(k) = 0.29$ for all $k > 0$. At $k = 0$, the scramjet is assumed to be operating in steady state with $\phi = 0.2$ at the inlet Mach number $M = 2.7$. Figure 2(a) shows the generated thrust with various filter choices. Note that the asymptotic value of the generated thrust can be arbitrarily chosen by varying the entries of N_1 and R_z. Figure 2(b) shows the corresponding values of equivalence ratios.

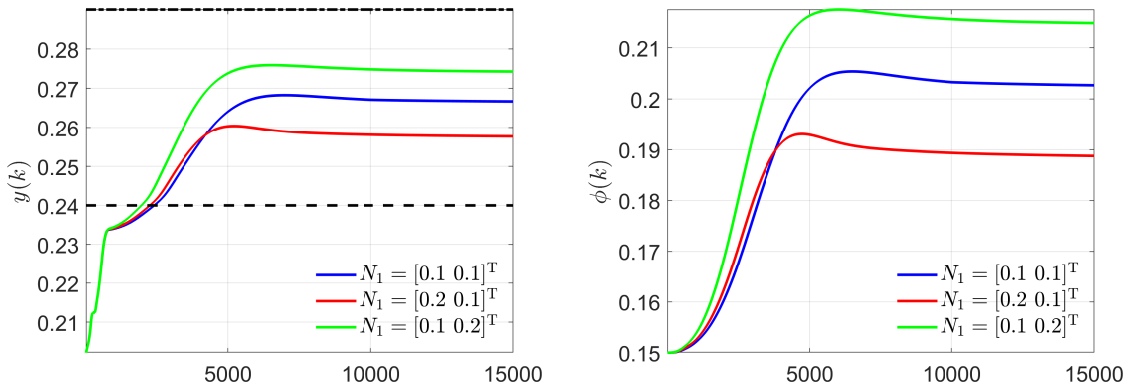

(a) Thrust

(b) Equivalence ratio

Figure 2: Closed-loop response of the scramjet to conflicting commands with various filter choices.

Motivated by the response of RCAC to conflicting commands, we introduce output constraints as additional commands to RCAC. As shown in the previous example, the output of the system varies linearly between the conflicting command, where the linear combination depends on the choice of the weights in RCAC. Thus, by selecting appropriate weights in RCAC, tradeoff between the output error and the constraint violation can be specified.

Consider the linear time-invariant system

$$x(k+1) = Ax(k) + Bu(k), \tag{2}$$

$$y(k) = Cx(k), \tag{3}$$

where

$$A \triangleq \begin{bmatrix} 0.41 & 0.17 & 0.65 \\ 0.18 & 0.34 & 0.29 \\ 0.14 & 0.77 & 0.02 \end{bmatrix}, \quad B \triangleq \begin{bmatrix} 0.19 \\ 0.24 \\ 0.56 \end{bmatrix}, \quad C \triangleq [0.43 \;\; 0.61 \;\; 0.04]. \tag{4}$$

Let $r = 1$. At steady state, the equilibrium state is given by

$$x_{\mathrm{eq}} = (I - A)^{-1}B(C(I - A)^{-1}B)^{-1}r = [1.18 \;\; 0.75 \;\; 0.84]^{\mathrm{T}}, \tag{5}$$

so that $Cx_{\mathrm{eq}} = r = 1$. It follows that $x(k) \to x_{\mathrm{eq}}$ if $y(k) \to r$ as $k \to \infty$. Now, consider the problem of constraining $x_3(k)$ to be less than 0.5. Thus, if $r = 1$, it follows from (5) that the constraint is violated in the case where $y(k) \to r$ as $k \to \infty$. RCAC is implemented with $N_1 = [5 \;\; 1]^{\mathrm{T}}$, $R_z = \mathrm{diag}(10, 1)$, $R_\theta = 10^2 I_{l_\theta}$, $R_1 = 2$, and $\lambda = 0.999$. Figure 3 shows the states and the constrained output of the system (2), (3). Note that the constraint is violated, but the constraint violation can be arbitrarily controlled by the choice of the weights in RCAC.

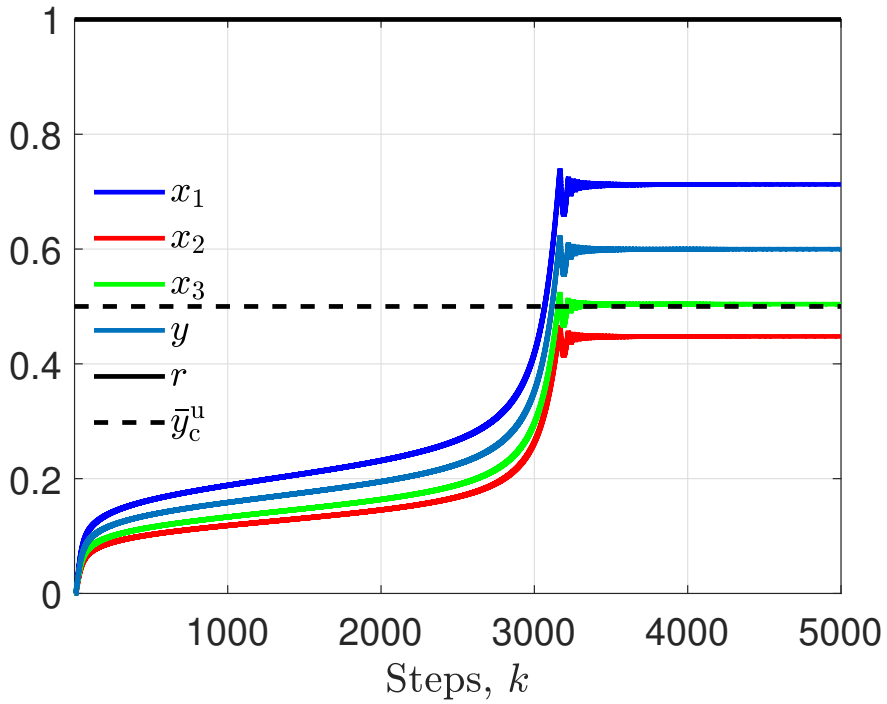

Figure 3: Closed-loop response of the system (2), (3) with auxiliary output constraints.

A major challenge in the operation of a scramjet is the need to prevent the scramjet from unstarting. When sufficient heat is released in the combustor, usually by means of too much fuel flow, the flow can thermally choke, resulting in a normal shock that travels upstream, thereby destroying the shock structure and the supersonic flow. Consequently, the thrust generated by the scramjet drops precipitously. This is usually fatal to the engine operation since it is extremely

difficult to establish a stable supersonic flow structure quickly enough once the engine has unstarted. In addition to excessive heat addition, a scramjet engine can unstart because of flow and structural perturbations. Because of unstart, there is an upper limit on the thrust that a scramjet engine can produce at a given operating condition.

To characterize the onset of unstart, we simulate the scramjet without feedback control for various fixed values of the equivalence ratio ϕ_0 at various constant inlet Mach numbers M_0 for 3000 time steps. At each M_0, if the applied equivalence ratio is less than the critical equivalence ratio, the scramjet reaches a stable equilibrium state and generates a constant thrust y_0 at the end of the simulation. If, however, the equivalence ratio is greater than the critical equivalence ratio, the state of the scramjet starts diverging as it attempts to establish a stable subsonic flow inside the scramjet, leading to a sharp loss of thrust. Figure 4(a) shows the asymptotic thrust y_0 for various values of constant equivalence ratios ϕ_0 at various constant inlet Mach numbers M_0.

In [6], a functional defined based on the pressure profile on the upper wall of the combustor is used to detect unstart. In [7], a single pressure measurement is used to detect and prevent unstart. Since the shock structure shifts longitudinally as the equivalence ratio is varied, the measured pressure can change sharply as the shock moves across the pressure sensor. Thus we use the mean p_{m} of the pressure along the bottom wall near the combustor to detect unstart. Specifically, 20 pressure sensors located uniformly between $x = 0.279$ m and $x = 0.294$ m are used to define the *pressure metric* p_{m}. This sensor arrangement corresponds to pressure measurements from 20 grid points in the simulation. Figure 4(b) shows the mean pressure p_{m} for various values of constant equivalence ratios ϕ_0 at various constant inlet Mach numbers M_0. Note that the mean pressure metric p_{m} increases abruptly once the scramjet unstarts due to the presence of a normal shock wave. Hence, the value of the metric p_{m} can be used to constrain the control algorithm to prevent the scramjet from unstarting.

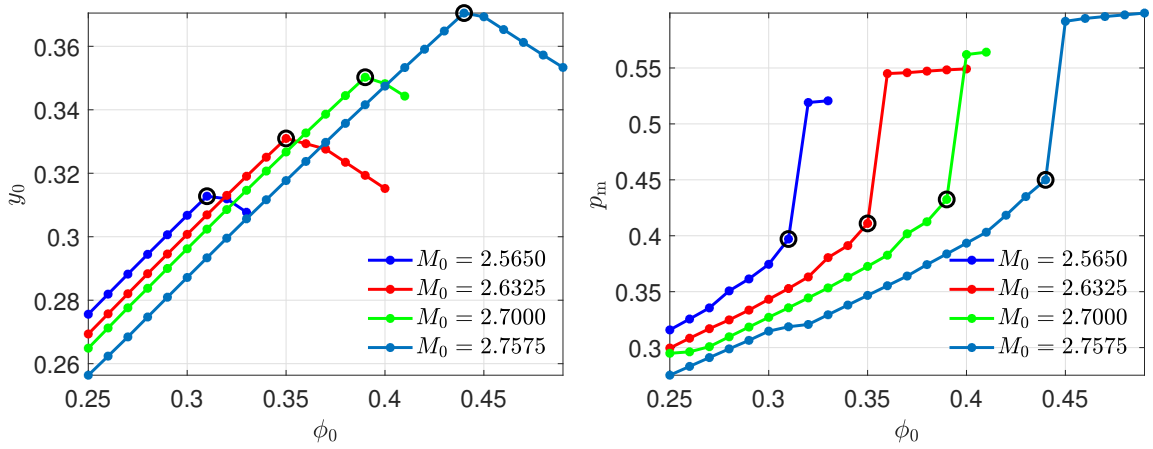

(a) Steady state Thrust

(b) Pressure Metric

Figure 4: Critical thrust y_0 and the pressure metric p_{m} in the normal operating and unstarting scramjet. The critical thrust at each value of M_0 is shown with a black circle.

Next, the closed-loop response of the scramjet with the auxiliary output constraint is considered, where the auxiliary output is the pressure metric p_{m}. Specifically, the constraint is given by

$$p_{\mathrm{m}}(k) \leq 0.4. \tag{6}$$

Note that $p_{\mathrm{m}} = 0.4325$ at the critical thrust $M_0 = 2.7$. The scramjet is commanded to follow the step command

$$r(k) = \begin{cases} 0.32, & k < 8000, \\ 0.355, & k \geq 8000. \end{cases} \tag{7}$$

At $k = 0$, the scramjet is assumed to be operating in steady state with $\phi_0 = 0.3$ at the inlet Mach number $M = 2.7$. RCAC is implemented with $N_1 = [1\ 1]^{\mathrm{T}}$, $R_z = I_2$, , $R_\theta = 10^7 I_8$, $R_1 = 1$, and $\lambda = 0.9999$.

For $k < 8000$, the commanded thrust is less than the critical thrust at the operating conditions, and thus the scramjet does not unstart and reaches a steady state. Note that $p_{\mathrm{m}} < 0.4$ for $k < 9000$, and thus the constraint is satisfied. For $k \geq 8000$, the commanded thrust is greater than the critical thrust at the operating conditions, thus the scramjet begins to unstart as the controller increases the equivalence ratio to increase the generated thrust. However, the constraint eventually becomes active, the scramjet converges to a steady state, and the output error and the constraint violation metric converge to constant values based on the choice of N_1, R_z, and R_1. Figure 5 shows the closed-loop response of the scramjet with auxiliary output constraint, (a) shows the measured output $y(k)$, (b) shows the equivalence ratio $\phi(k)$, (c) shows the constraint violation metric $z_1(k)$ and the output error $z_2(k)$, and (d) shows the coefficients of the controller optimized by RCAC.

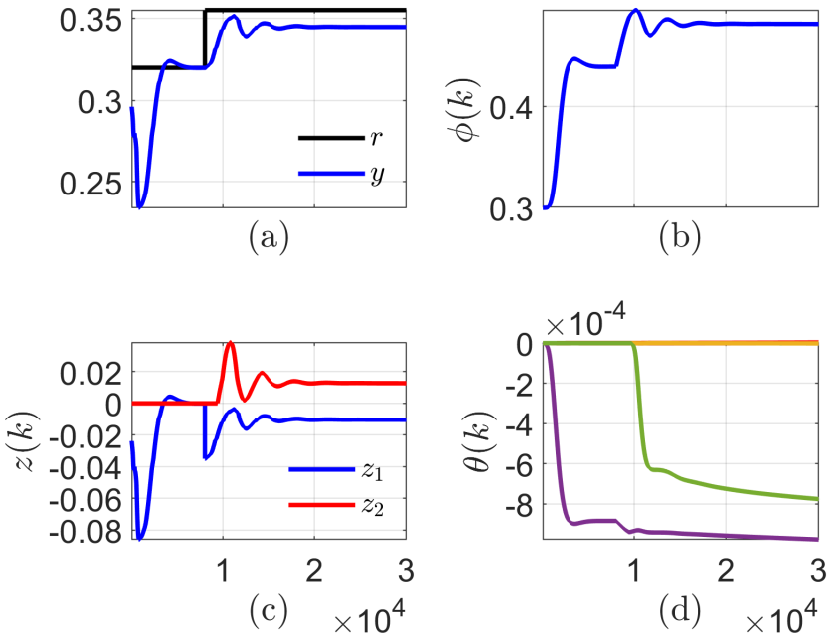

Figure 5: Closed-loop response of the scramjet with the auxiliary output constraint.

A supporting study on constrained PID control is under way.

2.2 RCAC-based PID Control

Motivated by the importance of PID control in applications, we extended RCAC to encompass PID control in [8]. The focus of this work was first-order systems with dead time, which is widely considered as the classical case for PID tuning. In particular, [8] presented a computational study to evaluate the performance and robustness of RCAC under off-nominal conditions involving nonlinearities, noise, and other effects.

2.3 Data-Driven RCAC (DRCAC)

In order to reduce the dependence on prior modeling, we have developed an extension of RCAC that uses recursive least squares (RLS) identification technique concurrently with the controller adaptation. To do this, we developed a technique that uses RLS to identify an infinite-impulse-response (IIR) model. The numerator coefficients (scalar or vector) are extracted from the model and used to update the target model used by RCAC (which is explained in [1]). We have demonstrated that this approach captures the nonminimum-phase (NMP) zeros of the plant sufficiently quickly

to prevent NMP pole/zero cancellation. This method is reported in [9], which includes applications to aerodynamic flutter and missile guidance.

3 Broader Impacts

This project supported the work of Dr. M. Kamaldar and the PI, leading to publications [5,7,8,9]. The developments under this project facilitated related efforts, including quadcopter flight tests as well as a proposal to UCAH on control of unstart in hypersonic vehicles.

References

[1] Y. Rahman, A. Xie, and D. S.. Bernstein. Retrospective Cost Adaptive Control: Pole Placement, Frequency Response, and Connections with LQG Control. *IEEE Contr. Sys. Mag.*, 37:28–69, Oct. 2017.

[2] M. A. Santillo and D. S. Bernstein. Adaptive Control Based on Retrospective Cost Optimization. *J. Guid. Contr. Dyn.*, 33:289–304, 2010.

[3] J. B. Hoagg and D. S. Bernstein. Retrospective Cost Model Reference Adaptive Control for Nonminimum-Phase Systems. *J. Guid. Contr. Dyn.*, 35:1767–1786, 2012.

[4] A. Ansari and D. S. Bernstein. Retrospective Cost Adaptive Control of the Generic Transport Model Under Uncertainty and Failure. *J. Aerospace Information Systems*, 14(3):123–174, 2017.

[5] A. Goel, K. Duraisamy, and Dennis Bernstein. Output-constrained adaptive control for unstart prevention in a 2D scramjet combustor. In *AIAA Scitech 2019 Forum*, page 0927, 2019.

[6] Q. Wang, K. Duraisamy, J. J. Alonso, and G. Iaccarino. Risk assessment of scramjet unstart using adjoint-based sampling methods. *AIAA J.*, 50(3):581–592, 2012. DOI: 10.2514/1.J051264.

[7] A. Goel, K. Duraisamy, and D. S. Bernstein. Retrospective Cost Adaptive Control of Unstart in a Model Scramjet Combustor. *AIAA Journal*, 56(3):1085–1096, 2018.

[8] Mohammadreza Kamaldar, Syed Aseem Ul Islam, Sneha Sanjeevini, Ankit Goel, Jesse B Hoagg, and Dennis S Bernstein. Adaptive digital pid control of first-order-lag-plus-dead-time dynamics with sensor, actuator, and feedback nonlinearities. *Advanced Control for Applications: Engineering and Industrial Systems*, 1(1):e20, 2019.

[9] Syed Aseem Ul Islam, Tam W. Nguyen, Ilya V. Kolmanovsky, and Dennis S. Bernstein. Data-Driven Retrospective Cost Adaptive Control for Flight Control Application. *Journal of Guidance, Control, and Dynamics*, 2021. to appear; also arXiv 2102.07191.